Double-Skin Facade Cavity Dynamics

Dan Bettenhausen
Jeff Vaglio
TJ DeGanyar

Standards for the structural design of dual-skin facade (DSF) curtain wall systems to resist wind load do not account for the geometric orientation of ventilation orifices with respect to the prevailing wind. Two numerical simulations of unsteady fluid dynamics are performed implementing the Shear Stress Transport (SST) turbulence model to predict the pressure exerted on the exterior barrier of a dual-skin facade under the condition of a transient wind for two different geometric configurations. It is determined that the orientation of the ventilation orifices produces a significant impact on the load carried by the outer wall. When designs create an air-flow path between the wind impingement surface and low pressure zones, such as the roof of the building, the load carried by the outer wall is much greater than the case where ventilation orifices are only placed at the impingement surface.
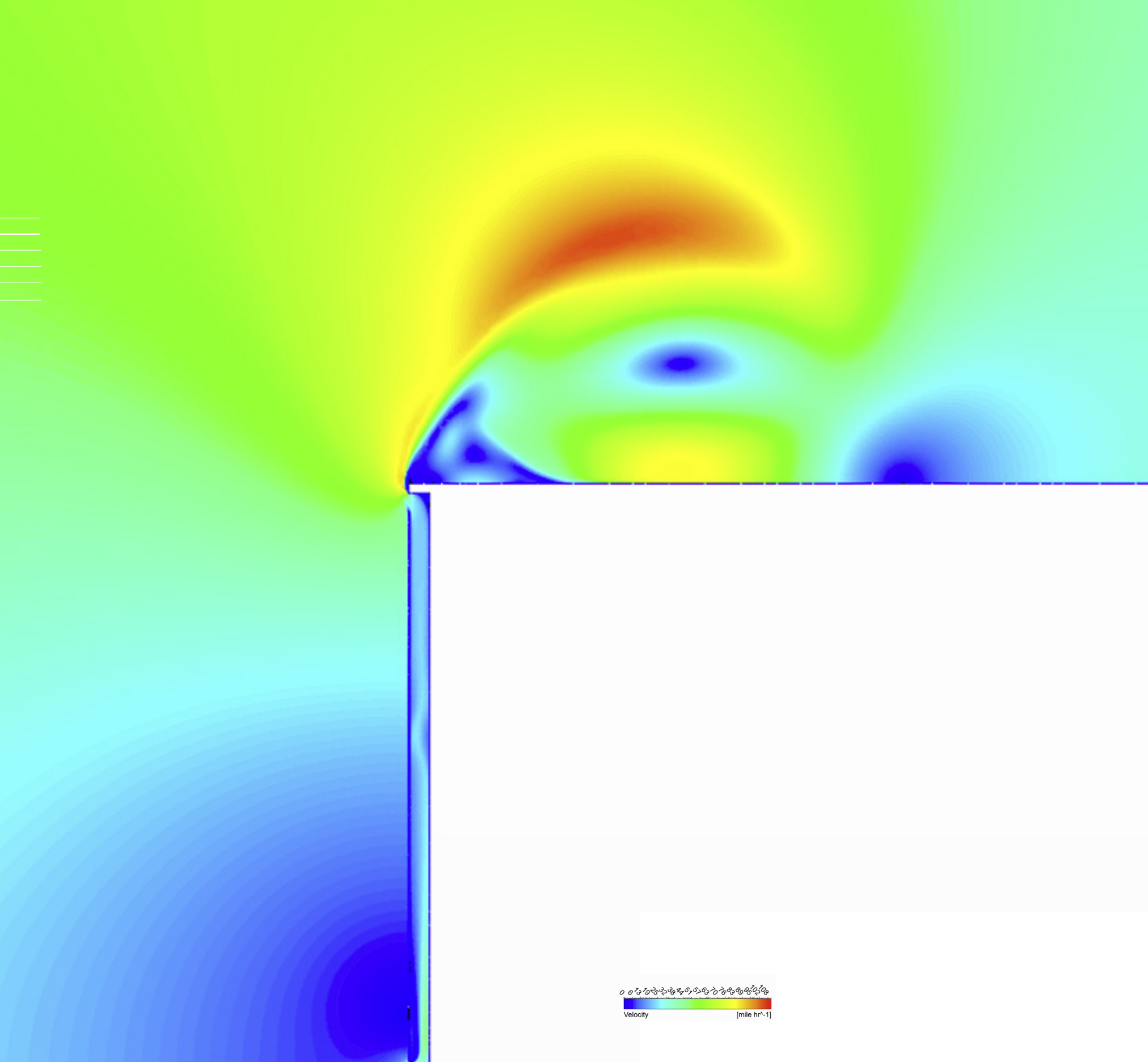
Velocity   [mile hr^-1]

A crucial requirement for the design of a curtain wall system is sufficient integrity to resist structural failure resulting from aerodynamic load. The long development history of standards implemented to prevent failure under predictable wind conditions bears an inalienable connection to the traditional single-wall construction of the building envelope.

In recent history designs have been proposed and implemented that utilize a multi-layered approach in order to harness benefits of increased energy efficiency, acoustic isolation and access to natural ventilation. The continued innovation of these technologies presents a need for revised structural standards that account for the fluid-dynamical interactions of wind with the multiple layers of the wall.

The primary emphasis of recent research is on the performance [1-4] and energy modeling [5-8] of double-skin facades. Investigation into the structural performance and pressure distributions of double-skin systems requires further exploration. Past research conducted in the area of pressure equalized rain screen (PER) design [9-13] and pressure equalized cavities [14-16] provides a precept for analysis of Multi-Layered Systems (MLS); however, the geometric scale and modes of ventilation associated with MLS configurations are more expansive and affect the load sharing between the internal and external skins. Recent research on the ballooning of flexible membranes [17] also has potential application to double-skin cavities with an exterior skin subject to large deformations, such as a cable-net facade. The structural flexibility of the interior and exterior skins affects the load sharing distribution of a double-skin.

The most pertinent research of pressure distributions includes Marques da Silva and Gloria Gomes [18] investigations of inner-face pressure distributions of multi-story DSF models obtained through wind tunnel tests for five wind incidences applied to four different systems with three gap depths, and Wellershoff and Hortmanns [19] wind tunnel study on DSF systems with gaps larger than 15 cm. The results of these investigations demonstrate

the sensitivity of pressure distribution in double-skin facades to project specific site conditions and design configurations. There is a need for a standardized procedure for the determination of loading on double-skin facade systems.

To the authors' knowledge there is currently a lack of standard guidelines addressing how to design and structurally analyze double-skin facades. Several attempts to document primary design considerations exist [20-21]; however determination of wind loading and load sharing of double-skins is addressed in brevity. Oesterle et al. acknowledge that the outer facade is primarily affected by short-term wind forces while the inner skin is subject to the steady components of wind [20], but variance in cavity geometry, opening configurations and airflow mode are not specified.

ASCE 7-05 Minimum Design Loads for Buildings and Other Structures Section 6.0 is void of consideration for multi-skin facades [22]. It is unclear how the definitions of partially enclosed building enclosure and air permeable cladding may relate to the determination of internal pressure coefficients for a double-skin which includes natural ventilation by operable units on the inner skin. The configuration of airflow openings is not addressed.

Eurocode EN-1991-1-4:2005 begins to present guidelines in Section 7.2.10 Pressure on walls or roofs with more than one skin [23]. This section specifies that the wind force on each skin is to be calculated separately. Section 7.2.10.3 identifies that the wind force on each skin is dependent on 1) the relative rigidity of the skins, 2) external and internal pressures, 3) distance between skins, 4) permeability of the skins and 5) the openings [23]. A series of rules are then presented for determining the pressure on each skin, but is restricted to a distance between skins less than 100 mm and where the "extremities of the layer between skins is closed". The presented rules are not applicable to configurations which put air into communication with other faces, excluding many double-skin facade airflow configurations. Researchers have concluded that the wind load guidelines established in Eurocode EN-1991-1-4:2005

require revision [18-19].

In the present work the pressure distribution and load sharing of multi-story DSF systems normal to prevailing winds is evaluated for multiple ventilation orifice configurations.

2   MULTI-STORY MODEL

Two geometric representations of a dual-facade system were investigated by the method of CFD.

Both cases represent the wind-facing wall of a low-rise building where the curtain wall is greater in its length dimension than its height dimension. In this case the flow can be regarded as two-dimensional, which greatly simplifies the solution domain and allows for liberal allocation of finite volumes to the solved space. The barriers of the DSF were modeled as rigid boundaries. This assumption is accurate when the outer wall implements traditional rigid framed units, but may not be applicable to the case where cable systems are used to suspend the outer wall. Both the three dimensional situation and the case where wall deflections are substantial provide opportunities for further research.

The solution domains observed in each case were similar and are depicted in Figure 1. The dimensions for each case are expressed in terms of the cross-sectional width of the orifices, which was specified to be 1 foot. The DSF configuration demarked as *Design A* features two orifices, both of which communicate to the air-impingement surface. A second case, that is labeled *Design B*, implements an alternate configuration where only one of the orifices is located normal to the prevailing wind. In this case, the second orifice is located at the roof of the building.

In both cases the wind is modeled as a transient with peak magnitude of 85 mph. The time-spatial variation is provided as Equation 1. The profile of the gust implements a power-law representation of the atmospheric boundary layer based on ASCE 7-05 for a 3 second time averaged wind gust with "suburban terrain" surface conditions. For this case the boundary

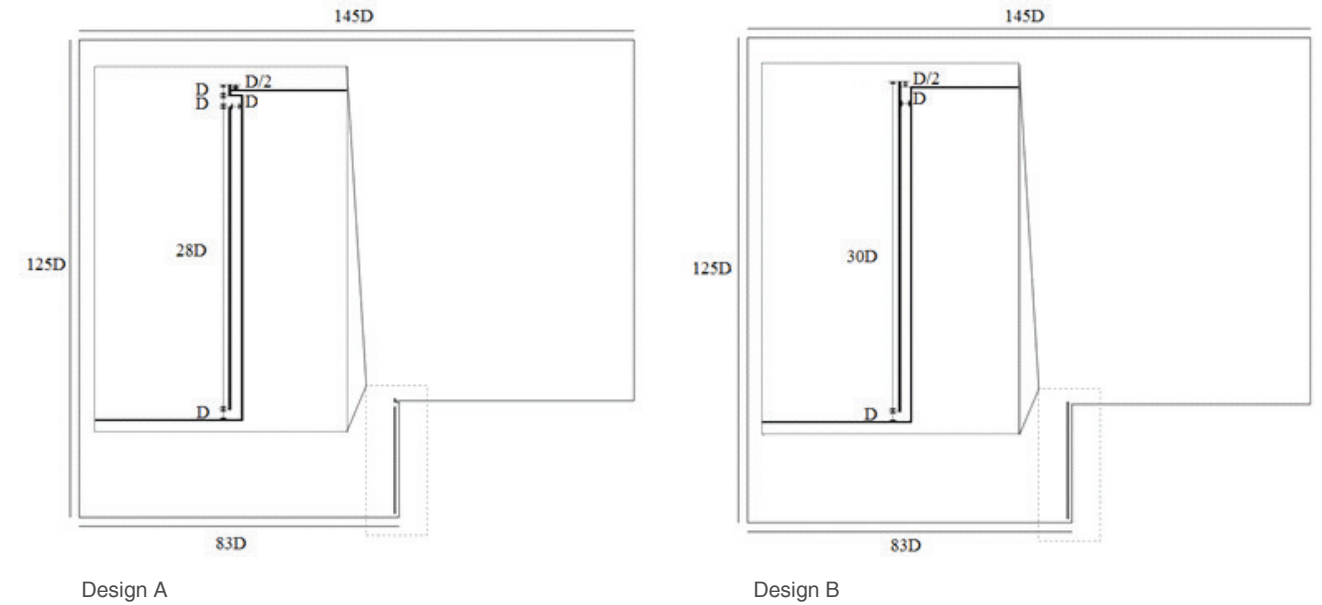Design A   Design B

Figure 1. Solution Domain and DSF Configurations Used in Simulation.

layer thickness is approximately 1200 ft and the model exponent is 1/7.

3   PHYSICAL MODEL

The governing equations of fluid mechanics implemented in the simulation are listed as Equations 2 through 5. Equation 2 represents the conservation of momentum in the form of the Incompressible Unsteady Reynolds Averaged Navier Stokes (U-RANS) equations for a tensor of order two, where j_1 represents the dimension normal to the wall surface and j_2 represents the

dimension parallel to the wall surface. This convention is used in all of the cited equations. Equations 3 and 4, the Shear Stress Transport (SST) equations of Menter [24], prescribe the Reynolds Stress by solution of the turbulent viscosity field. Equation 3 dictates the conservation of turbulence production and Equation 4 provides for conservation of turbulence dissipation. Equation 5 is the well known continuity equation.

CFX commercial software was implemented to obtain the approximated numerical solution by finite volume method. A flux limited second order upwinding scheme

was implemented for Equations 2 and 5 while a first order unwinding was implemented for Equations 3 and 4. Grid cell allocation was controlled to maintain a fine grid at wall boundaries.

Time marching was performed via the 2nd order backward Euler method and multiple linearizations were performed at each time level to maintain a convergence value of 10e-5 for the rms average of the residuals at each cell corresponding to each conservation equation. Numerical accuracy was also assessed by utilizing multiple grid levels. Models were investigated at both 260,000 and 385,000 cells. There was no appreciable change in the result.
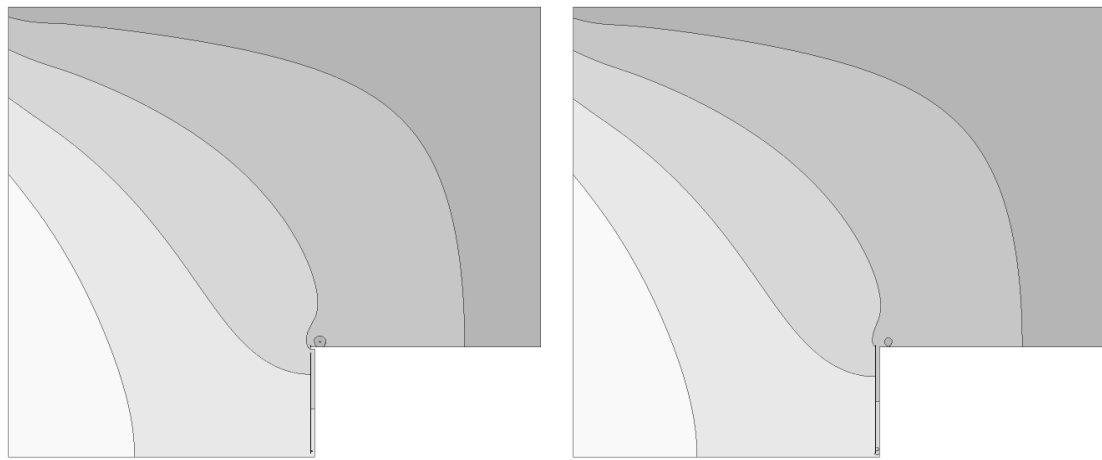
[1] $u_i(y,t) = 85 \sin\left(\frac{\pi t}{3s}\right)\left(\frac{y}{1200}\right)^{\left(\frac{1}{7}\right)} mph \quad t(0,3)$

[2] $\frac{\partial \rho u_j}{\partial t} + \rho\left(u_i \frac{\partial u_j}{\partial x_i}\right) = -\frac{\partial p}{\partial x_j} + \frac{\partial}{\partial x_i}\left((\mu + \mu_t)\frac{\partial u_j}{\partial x_i}\right) \quad j = 1,2$
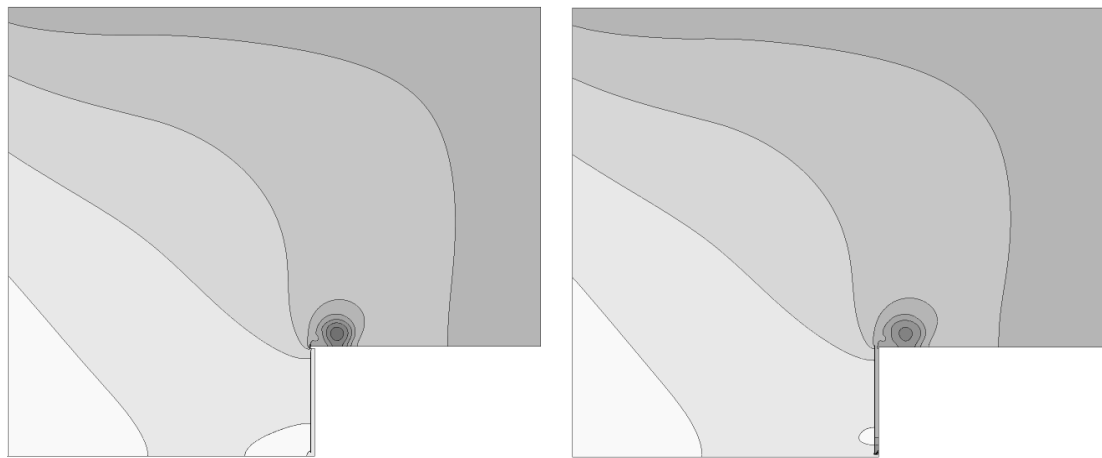
[3] $\frac{\partial \rho \kappa}{\partial t} + \frac{\partial(\rho u_i \kappa)}{\partial x_i} = P_\kappa - \beta_1 \rho \kappa \omega + \frac{\partial}{\partial x_i}\left[\left(\mu + \frac{\mu_t}{\sigma_\kappa}\right)\frac{\partial \kappa}{\partial x_i}\right]$

[4] $\frac{\partial \rho \omega}{\partial t} + \frac{\partial(\rho u_i \omega)}{\partial x_i} = A \rho S^2 - \beta_2 \rho \omega^2 + \frac{\partial}{\partial x_i}\left[\left(\mu + \frac{\mu_t}{\sigma_{\omega_1}}\right)\frac{\partial \omega}{\partial x_i}\right] + 2(1 - F_1)\rho \frac{1}{\sigma_{\omega 2}\omega}\frac{\partial \kappa}{\partial x_i}\frac{\partial \omega}{\partial x_i}$
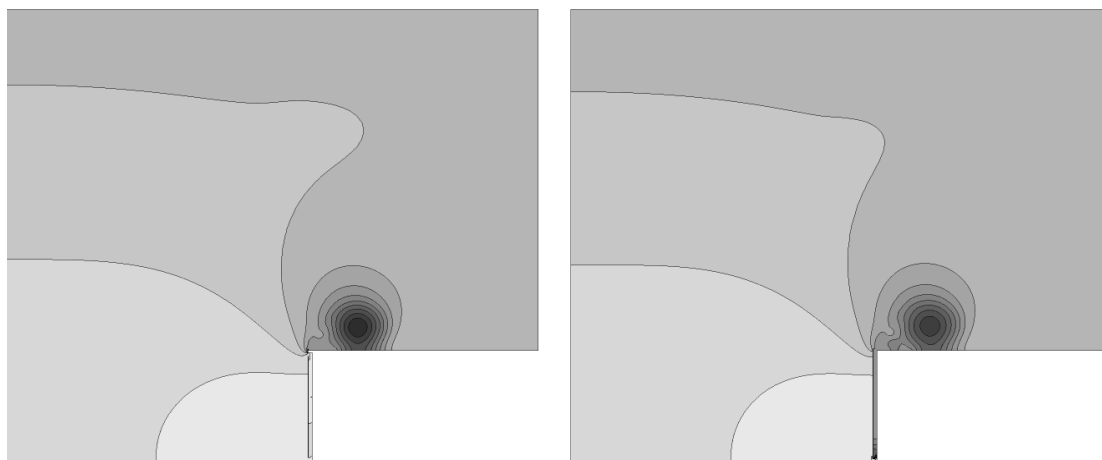
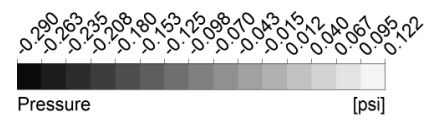[5] $\frac{\partial \rho}{\partial t} + \frac{\partial \rho u_j}{\partial x_i} = 0$

t = 0.5 s

t = 1 s
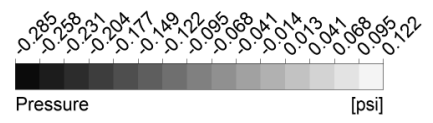
t = 1.5 s

-0.290	-0.263	-0.235	-0.208	-0.180	-0.153	-0.125	-0.098	-0.070	-0.043	-0.015	0.012	0.040	0.067	0.095	0.122					

Pressure   [psi]

Design A

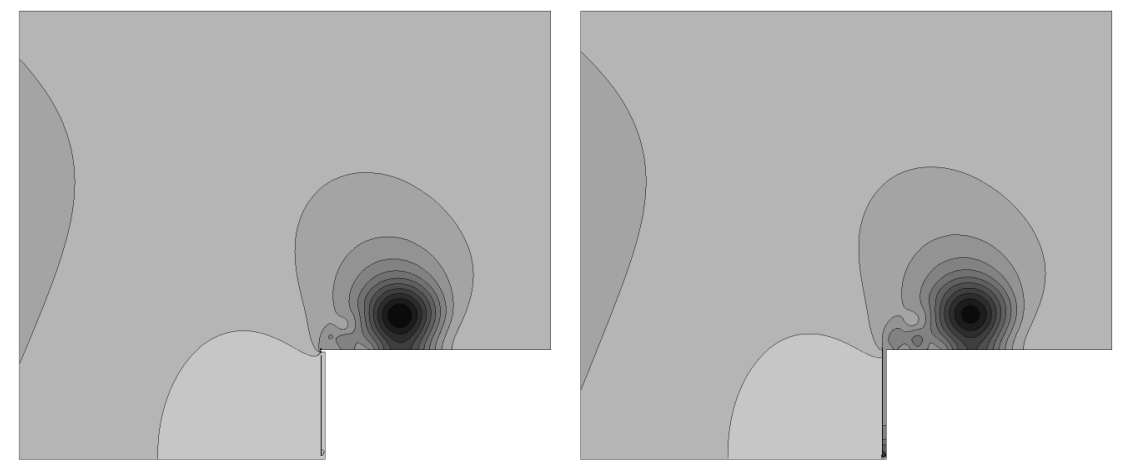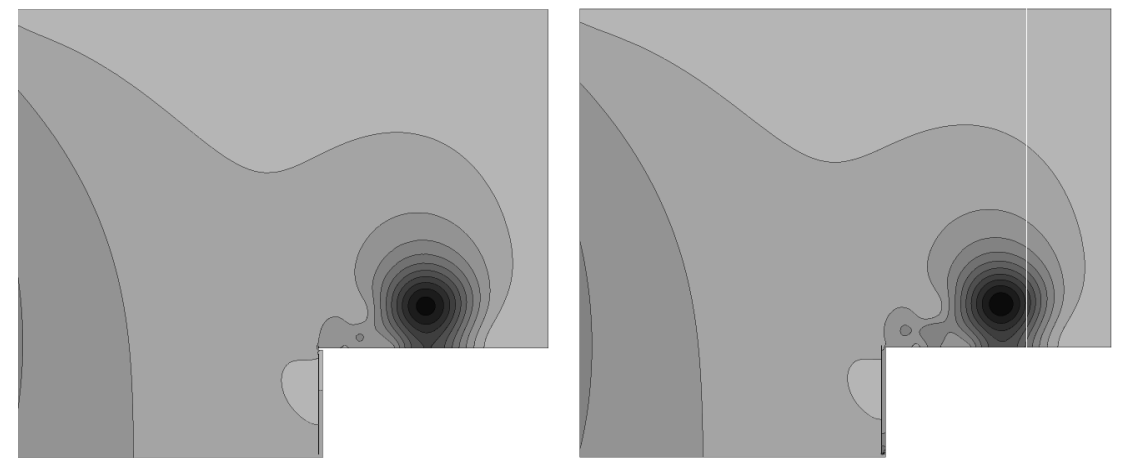|																
-0.285	-0.258	-0.231	-0.204	-0.177	-0.149	-0.122	-0.095	-0.068	-0.041	-0.014	0.013	0.041	0.068	0.095	0.122

Pressure   [psi]

Design B
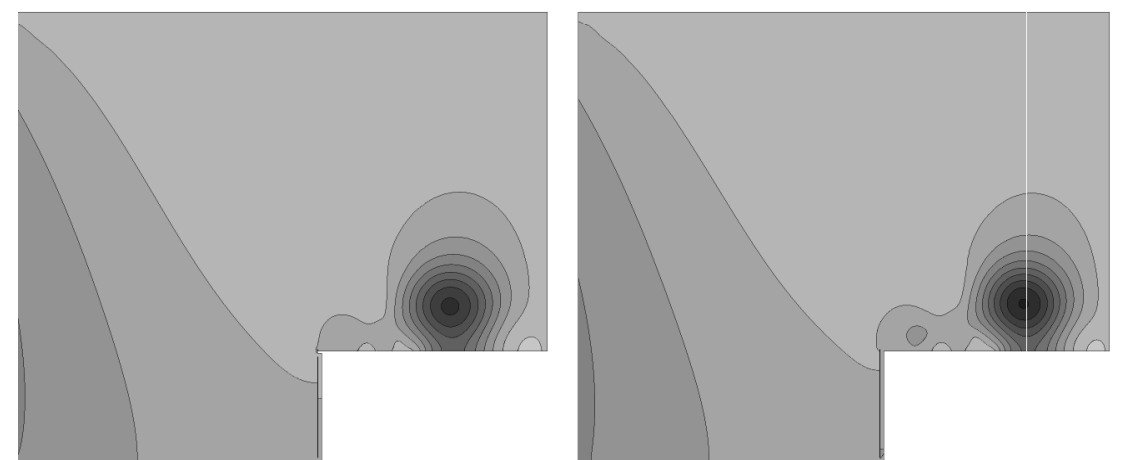
Figure 2. Pressure distribution for Design A (left) and Design B (right) at various times.

t = 2 s

t = 2.5 s

t = 3 s

-0.290	-0.263	-0.235	-0.208	-0.180	-0.153	-0.125	-0.098	-0.070	-0.043	-0.015	0.012	0.040	0.067	0.095	0.122

Pressure   [psi]

Design A

-0.285	-0.258	-0.231	-0.204	-0.177	-0.149	-0.122	-0.095	-0.068	-0.041	-0.014	0.013	0.041	0.068	0.095	0.122

Pressure   [psi]
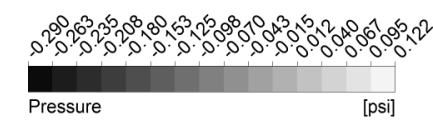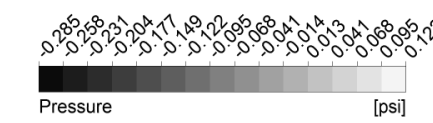
Design B

Figure 2 (continued). Pressure distribution for Design A (left) and Design B (right) at various times.

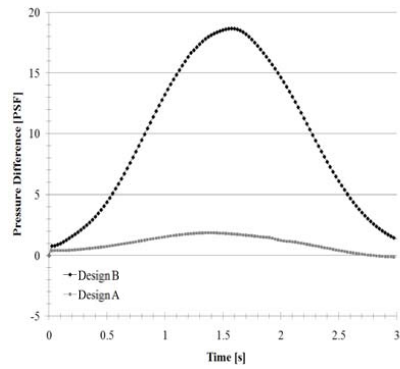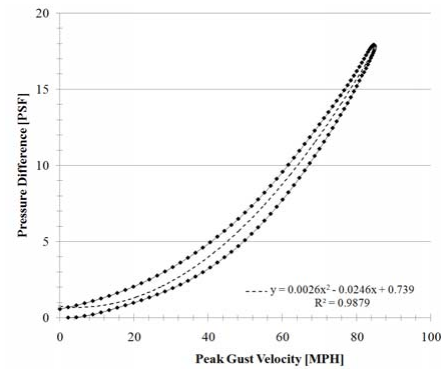Figure 3. Outer Skin Averaged Pressure Difference versus Time

Figure 4. Outer Skin Averaged Pressure Difference versus Peak Gust Velocity

4   BOUNDARY CONDITIONS

The vertices of the solution domain are labeled A through D and the surfaces of the curtain wall fall within the zone annotated by E in Figure 1. At the solution boundary AB velocity is specified by Equation 1 and the resulting pressure distribution is variable. The locations BC and CD are specified pressure and entrainment conditions where a pressure of zero gauge to the initial domain pressure is specified to be invariable with time and the second derivative of velocity is constrained to zero. At the boundaries extending into the zone of location E and all surfaces within that zone are walls and the no-slip condition is enforced.

5   RESULTS AND DISCUSSION

In order to produce standards that prescribe appropriate pressure correlations to the free stream air velocity it is necessary to predict how the ventilation of the DSF affects its fluid-dynamic scenario of operation and the resulting pressure variations over its surfaces.

Figure 2 shows the pressure distribution of the solution domain at discrete points in time. It can be observed that the pressure response of the internal cavity that is formed between the walls of the DSF to the simulated wind condition is different for the two cases studied. An implication of this fact is that structural design requirements would not be the same for both systems.

In the case of Design A the variation in pressure over the outer impinged surface of the wall is small with respect to the difference between the mean pressure over the surface and the ambient pressure.

Since both of the ventilation orifices in the external wall connect to this zone, the cavity pressure is relatively uniform and equal to that of the impingement zone. Since a small change in pressure does occur due to boundary layer development along the surface a mild airflow does take place in the cavity.

The situation of Design B strongly contrasts the alternate configuration investigated. It is well established that the leading corner of the building will result in the development of a free shear layer which may exhibit instability in the form of vortex shedding or other aerodynamic phenomena. Air entrained by this layer may gather sufficient rotational velocity to generate a low pressure zone at the roof of the building. The ventilation mode implemented in this situation provides communication between this low pressure region and the higher pressure of the impingement surface resulting in acceleration of air in the cavity and a reduction in cavity pressure.

Figure 3 provides a comparison of the load at the outer barrier for both designs. Since the wall is rigid the net force is proportional to the difference in the area-average of pressure at its surfaces. In the case of Design A there is very little pressure difference acting across the outer wall, while in the case of Design B the pressure difference is substantial.

In the case of Design B, where the wind load is appreciable, the area-averaged pressure difference was found to scale to the second power of the peak air velocity in a manner similar to the calculation of stagnation pressure for a given velocity by ASCE 7-05. This result is provided in Figure 4.

6   CONCLUSION

The results obtained in this study bear obvious implications for the design of DSF systems; namely, that the ventilation geometry can have a substantial impact on the structural design requirements for the exterior layer. Analysis of the transient condition indicated that for the specific case in question, that the loading of the outer wall bared a relationship similar to that of the ASCE 7-05 method.

REFERENCES

[1] Gratia, E. & Herde, A. (2007) "The most efficient position of shading devices in a double-skin facade", Energy and Buildings, 39, pp. 364–373.

[2] Jiru, T.E. & Haghighat, F. (2008) "Modeling ventilated double skin facade - A zonal approach", Energy and Buildings, 40, pp. 1567–1576.

[3] Manz, H. & Frank, T. (2005) "Thermal simulation of buildings with double-skin facades", Energy and Buildings, 37, pp. 1114–1121.

[4] Tanaka, H.; Okumiya, M.; Tanak, H.; Yoon, G.Y.; Watanabe, K. (2009) "Thermal characteristics of a double-glazed external wall system with roll screen in cooling season", Building and Environment, 44, pp. 1509-1516.

[5] Guardo, A.; Coussirat, M.; Egusquiza, E.; Alavedra, P.; Castilla, R. (2009) "A CFD approach to evaluate the influence of construction and operation parameters on the performance of Active Transparent Facades in Mediterranean climates", Energy and Buildings, 41, pp. 534-542.

[6] Hensen, J.; Bartak, M.; Frantisek, D. (2002) "Modeling and simulation of a double-skin facade system", ASHRAE Transactions, 108(2), pp. 1251–1259.

[7] Manz, H. (2004) "Total solar energy transmittance of glass double facades with free convection", Energy and Building, 36, pp. 127–136.

[8] Saelens, D.; Carmeliet, J.; Hens, H. (2003) "Energy Performance Assessment of Multiple Skin Facades", International Journal of HVAC&R Research, 9(2), pp.167-186.

[9] Suresh Kumar, K. & Wisse, J.A. (2001) "Pressure equalization of rainscreen facades: Analysis of the field data in the frequency domain", Wind and Structures, 40(2), pp. 101-118.

[10] Baskaran, A. (1994) "A Numerical Model to Evaluate the Performance of Pressure Equalized Rainscreen Walls", Journal of Building and Environment, 29(2) pp.159-171.

[11] Choi, E.C.C. & Wang, Z. (1998) "Study on pressure-equalization of curtain wall systems", Journal of Wind Engineering and Industrial Aerodynamics, 73(3), pp. 251-266.

[12] Inculet, D.R., & Davenport, A.G. (1994) "Pressure-equalized rainscreens: A study in the frequency domain", Journal of Wind Engineering and Industrial Aerodynamics, 53, pp. 63-87.

[13] Quirouette, R.L. & Rousseau, J. (1998) "A review of pressure equalization and compartmentalization studies of exterior walls for rain penetration control", Water Leakage Through Building Facades, ASTM STP, 1314, pp. 47-56.

[14] Sharma, R.N. (2007) "Internal and Net Envelope Pressures in a Building having Quasi-static Flexibility and a Dominant Opening", Journal of Wind Engineering and Industrial Aerodynamics, 96(6-7), pp. 1074-1083.

[15] Xie, J.; Schuyler, G.D.; Resar, H.R. (1992), "Prediction of net pressure on pressure equalized cavities", Journal of Wind Engineering and Industrial Aerodynamics, 41-44, pp. 2449-2460.

[16] van Schijndel, A.W.M. & Schols, S.F.C. (1998) "Modeling pressure equalization in cavities", Journal of Wind Engineering and Industrial Aerodynamics, 74-76, pp. 641-649.

[17] Shi, X. & Burnett, E. (2008), 'Mechanics and test study of flexible membranes ballooning in three dimensions', Building and Environment, 43(11), pp. 1871-1881.

[18] Marques da Silva, F. & Gloria Gomes, M. (2008) "Gap inner pressures in multi-storey double skin facades", Energy and Buildings, 40, pp. 1553-1559.

[19] Wellsershoff, F. & Hortmanns, M. (1999) "Wind loads on double facade systems with gaps greater than 15 cm", in Proceedings of the Wind Engineering into the 21st Century, Balkema Publishers, Copenhagen, Denmark.

[20] Oesterle, E.; Lieb, R.D.; Lutz, M.; Heusler, W. (2001) Double-Skin Facades – Integrated Planning, Prestel, Munich, Germany.

[21] Bestfacade (2007) "WP 5 Report Best Practice Guidelines", Best Practice for Double Skin Facades, Blomsterberg, A (ed.), Intelligent Energy Europe.

[22] ASCE/SEI 7-05 (2006) Minimum Design Loads for Buildings and Other Structures, American Society of Civil Engineers, Reston, Virginia.

[23] CEN/TC250 (2005) Eurocode 1 Part1-4 Actions on structures: General actions: Wind Actions, EN 1991-1-4:2005 (E).

[24] Menter (1994) "Two-equation eddy-viscosity turbulence models for engineering applications", AIAA Journal, 32(8), pp. 1598–1605.